EFFECT OF METAL INSERTION ON THE HYDROGEN STORAGE PROPERTIES OF CARBON NANOFIBERS PREPARED BY ELECTROSPINNING

Mehraj-ud-din Naik, Jong Gu Kim, Ji Sun Im and Young-Seak Lee

Department of Applied Chemistry and Biological Engineering, Chungnam National University, Daejeon, 305-764, Republic of Korea

Introduction

Carbon nanostructures are considered one of the best options for the storage of hydrogen due to their high surface area, low density, low cost, and easy to handle [1]. In particular, carbon nanomaterials such as carbon nanotubes, fullerenes, and carbon nanofibers (CNFs), due to their large surface area, have attracted much attention as molecular hydrogen storage materials to meet DOE's 2015 hydrogen storage target [2]. Storage capacities ranging from 0.25 to 20 wt % have been reported [3], and numerous factors have been used to describe the variability and inconsistency of these results, including sample preparation, processing conditions and presence of impurities such as amorphous carbon and catalyst particles. The noble metal nanoparticles (including Pd, Pt, Ti, and Ag) have been applied on CNT support and examined in selective hydrogenation reactions [4]. The metal embedded carbon nanomaterials have shown interesting results with improved applications in varied fields including hydrogen storage, lithium batteries etc. as compared to as pristine carbon nanostructures [5]. Metal or metal oxide embedded carbon nanostructures provide a wide range of properties with convincing surface morphologies particularly essential for the high hydrogen storage capacities.

Experimental

Polyacrylonitrile (PAN), and N, N-Dimethylformamide (DMF) 99.5% were purchased from Aldrich and were used without further purification. The metal catalysts used such as Manganese powder 99+%, and Titanium Oxy sulfate (TiOSO$_4$) were obtained from Aldrich. Vanadium (V) Oxide (V$_2$O$_5$) 99.0%, was procured from Junsei chemicals respectively, and were used without any purification except Mn which was paint shacked for 1 h to reduce its particle size. The mass fraction of 12% PAN/DMF homogeneous solution was prepared by mixing and stirring at70℃ for 5 to 10 h. The each metal catalyst (5 wt. % metal based) was dissolved in DMF for few hours at 50℃ with constant stirring. The prepared catalyst solution was added to the PAN solution slowly with continuous stirring to get a uniform or homogenous solution. The chemical composition for the preparation of each sample is given in Table I

The CNFs were prepared through an electrospinning method with a sophisticated current control attached having a capacity of 60 kV producing current. In addition an electrospun fiber collector is kept at a certain distance from the tip (10-15cm) and directed towards each other. The current passing through the circuit generates an electronic field which gives rise to the small fibers from the tip of a syringe containing the polymer solution.

Metal/PAN-based fibers (Metal = Mn, Ti, V) were prepared by electrospinning a polymer/metal precursor solution containing both the desirable contents of metal (wt.% of metal maintained to 5) and a 12 wt.% PAN polymer solution dissolved in DMF. The amount of metal precursors used was limited to 5 wt.% in all cases. The precursors used for Ti, V, and Mn metals were TiOSO$_4$, V$_2$O$_5$, and Mn Powder, respectively. The ratio of the PAN polymer and the metal content in the electrospun solution was maintained approximately 16:1 respectively.

Results and Discussion

XPS is an effective tool to reveal out chemical state of modified metal atoms on the CNFs. Change in binding energy of carbon or oxygen elements by the modifications is helpful to deduce the incorporation scheme of metal atoms. The core level analysis of all prepared samples was carried out by using an XPS technique as shown in Fig.1. The XPS spectrum of raw CNF exhibited two major states as C1s and O1s as indicated in trace 'a' of Fig.1. However the Fig.1 (b-d) exhibited Ti2p, V2p, and Mn2p states respectively, in addition to C1s and O1s states which are also the main characteristic features of the XPS spectrum in Fig.1a. The Binding energy of C1s peak of the CNF is 284.5 eV and was not altered by titanium modification, while O1s peak of CNF-Ti became broad with binding energy 532.0 eV indicates the adsorption of hydroxyl groups [6] believed to come from the atmospheric moisture. However this binding energy of O1s reveals that there is negligible or no Ti-O bonding in CNF-Ti, but that for oxygen atoms bonded with metal atoms is 530.5 eV [7]. In addition the increase in O1s peak at low energy side by the vanadium and manganese insertion in Fig.1(c and d) suggested that the part of oxygen atoms was bonded to vanadium and manganese atoms producing V-O and Mn-O bonds respectively. This observation was confirmed by XRD analysis.

The adsorption in CNF-Ti was completed at a lower pressure of P/P$_0$ < 0.03 and gives formation of a sharply inclined knee at P/P$_0$ < 0.03. This narrow knee formation indicates that the sample has a micropore size distribution which is clearly shown in Fig.2. However it is also important to mention that all the samples in addition to micropores also possess mesopores as observed in Fig.2. The isotherms correspond to a type I (IUPAC classification) associated with the presence of both micropores and mesopores are reported to have no effect on the curve once the micropores are filled at low relative pressure (P/P0 < 0.03), the adsorption becomes significant on the surfaces contains mesopores to be indicated by the slope at higher relative pressures.

The BET results suggested that, during the pore development, there were different pore opening mechanisms operating on the metal inserted CNFs activated using the KOH

solution. Furthermore, the BET surface area for all metal embedded CNF samples showed interesting results supporting the XRD, FESEM investigations. The BET surface area for CNF-Ti (1574 m^2g^{-1}) and CNF-Mn (1452 m^2g^{-1}) is approximately 3 times higher than that of CNF-V (543.5 m^2g^{-1}) and CNF (638 m^2g^{-1}) sample. The higher surface area might be due to the larger pore volume of CNF-Ti and CNF-Mn, which is related to the higher degree of dispersion and size of titanium and manganese (note that Mn powder size was reduced by paint shaker prior to its addition in PAN) on the CNFs than that of vanadium embedded CNFs.

Finally the differences in the porosity-viz-surface area of the metal embedded CNFs which were discussed above are depending on many factors from activation process through alkoxides to catalytic effect of different metals used. The best metal in order to increase specific surface area as well as porosity is believed to be titanium and manganese due to their excellent dispersion as well as the catalytic effect on the carbon nanofibers surfaces. The V metal used as catalysts on CNFs has ordinary effect on the CNFs surfaces due to their low dispersion as well as larger size as an oxides or composites formed.

Table 1. Composition of Prepared Samples in this Study.

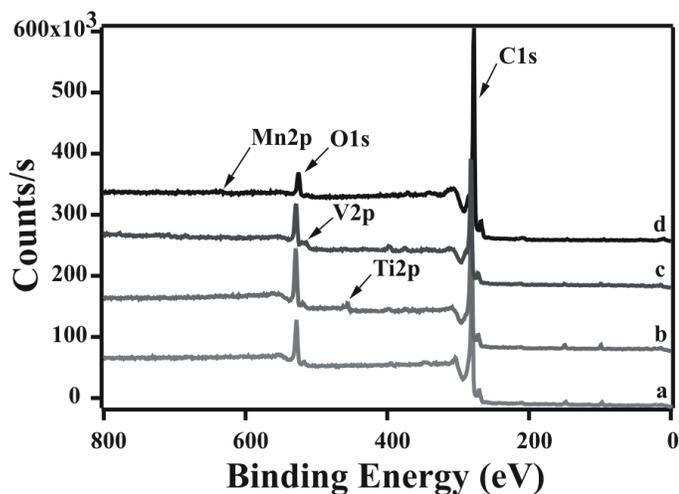| Sample name	Solvent (DMF) g	PAN (g)	Catalyst (wt.%)
CNF	29	4	-
CNF-Ti	29	4	5
CNF-V	29	4	4.85
CNF-Mn	29	4	5

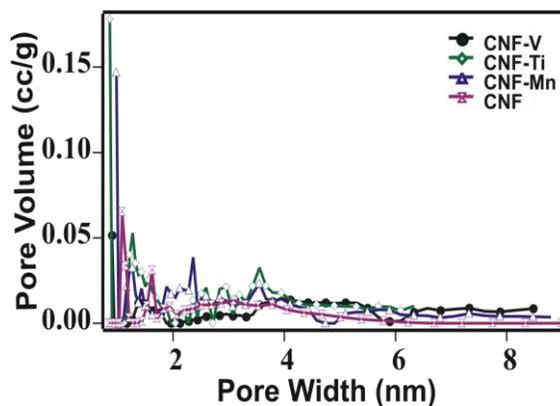**Fig.1** XPS spectra of; a CNF, b CNF-Ti, c CNF-V, and d CNF-Mn.

Fig. 2 Pore size distribution of samples.

Conclusions

In summary we have demonstrated the comparative study of carbon nanofibers and metal embedded carbon nanofibers and their hydrogen storage properties were discussed. The BET analysis of prepared samples showed improved surface morphology and porosity after carrying out KOH activation process. The best catalysts in order to improved surface morphology and hydrogen storage capacity were found to be Ti and Mn which showed approximately 2.8 and 1.6 wt.% of hydrogen storage capacity respectively, at 77K and 9MPa. These results were also supported by the BET analysis of prepared sample where CNF-Ti and CNF-Mn with specific surface area 1572 and 1452 m^2g^{-1} respectively, showed improved micropore volume and pore properties as compared to CNF-V and raw CNF with surface area 543 and 638 m^2g^{-1} respectively. The effect of these metals on CNF surfaces was evident after obtaining an enhanced hydrogen storage capacities and properly investigating the BET results.

References
[1] Dillon AC, Jones KM, Bekkedahl TA, Kiang CH, Bethune DS, Heben MJ. Storage of hydrogen in single-walled carbon nanotubes. Nature 1997;386:377-379.
[2] Coontz R, Hanson B. Not so simple. Science 2004;305:957.
[3] Yurum Y, Taralp A, Vezirolugo TN. Storage of hydrogen in nanostructured carbon materials. Int J Hydrogen Energy 2009;34:3784-3798.
[4] Rather SU, Zacharia R, Hwang SW, Naik MUD, Nahm KS. Hyperstoichiometric hydrogen storage in monodispersed palladium nanoparticles. Chem Phys Lett 2007;438:78–84.
[5] Kamat PV. Carbon nanomaterials: Building blocks in energy conversion devices. Interface 2006;15:45-47.
[6] Ryoo MW, Seo G. Improvement in capacitive deionization function of activated carbon cloth by titania modification. Water Research 2003;37:1527-34.
[7] Kumar PM, Badrinarayanan S, Sastry M. Nanocrystalline TiO_2 studied by optical, FTIR and X-ray photoelectron spectroscopy: correlation to presence of surface states. Thin Solid Films 2000;358:122-130.